

## Fullerenium Salts: A New Class of C<sub>60</sub>-Based Compounds

Mauro Riccò,<sup>\*,†</sup> Daniele Pontiroli,<sup>†</sup> Marcello Mazzani,<sup>†</sup> Fabio Gianferrari,<sup>†</sup>  
Massimo Pagliari,<sup>†</sup> Angelo Goffredi,<sup>†</sup> Michela Brunelli,<sup>‡</sup> Giorgia Zandomeneghi,<sup>§</sup>  
Beat H. Meier,<sup>§</sup> and Toni Shiroka<sup>||</sup>

*Dipartimento di Fisica, Università di Parma, Via G. Usberti 7/a, 43100 Parma, Italy, Institut Laue Langevin, BP 156, 6, rue Jules Horowitz, 38042 Grenoble Cedex 9, France, Physical Chemistry Laboratory, ETH-Zurich, Wolfgang-Pauli-Strasse 10, CH-8093 Zurich, Switzerland, and Laboratorium für Festkörperphysik, ETH-Zurich, Schafmattstrasse 16, CH-8093 Zurich, Switzerland*

Received November 12, 2009; E-mail: Mauro.Ricco@fis.unipr.it

**Abstract:** We report here on the preparation and characterization of a fullerenium salt in the solid state, where the fullerene is in the 2+ oxidized state. To succeed in this long-standing challenge, we exploit the oxidizing power of one of the strongest Lewis acids, AsF<sub>5</sub>. The weak nucleophilic character of its conjugate base is essential in stabilizing the fullerene dication in a crystal lattice. High-resolution structural analysis of this compound, with the formula C<sub>60</sub>(AsF<sub>6</sub>)<sub>2</sub>, indicates that the highly reactive C<sub>60</sub><sup>2+</sup> units are arranged according to a novel 1D “zigzag” polymer structure. The molecules are connected by an alternating sequence of four-membered carbon rings ([2 + 2] cycloaddition) and single C–C bonds. The long awaited high-T<sub>c</sub> superconductivity and magnetism, expected in a hole-doped C<sub>60</sub> compound, are replaced instead by a semiconducting behavior, quite probably originating from the reduced crystal and molecular symmetry upon polymerization. The small value of the energy gap (approximately 70 meV) suggests, nevertheless, the proximity of a metallic phase.

### 1. Introduction

The large variety of compounds referred to as fullerides are intensively investigated due to their exciting electronic and transport properties, such as high-T<sub>c</sub> superconductivity, molecular magnetism, and ionic conductivity.<sup>1–6</sup> These C<sub>60</sub> charge-transfer salts invariably contain C<sub>60</sub> in its anionic form. In fact, the observation of six reversible reduction states<sup>7</sup> confirms that C<sub>60</sub> is an exceptionally good electron acceptor but, consequently, also a bad electron donor. However, the interest in producing a fullerenium salt, namely, a solid in which the fullerenes are in the oxidized state, is kept rather high, prompted by the noticeable electronic properties expected in a “hole-doped” C<sub>60</sub> compound.<sup>8–10</sup>

Although the oxidation of C<sub>60</sub> has already been reported in the gas phase<sup>11</sup> and in solution,<sup>12</sup> the preparation of an ionic solid containing C<sub>60</sub> as a cation has proved to be quite a challenging task, due to the extreme reactivity of the C<sub>60</sub><sup>n+</sup> species. Here, we report on the synthesis and the extensive characterization of the compound C<sub>60</sub>(AsF<sub>6</sub>)<sub>2</sub>, where fullerenes are in the 2+ oxidized state. We show that in this system the extremely reactive C<sub>60</sub><sup>2+</sup> cations, among the most reactive molecular ions in nature, organize themselves to form a novel 1D polymer architecture. Nuclear magnetic resonance (NMR), SQUID magnetometry, and dc conductivity show that this polymer is a diamagnetic semiconductor. These results establish a new class of C<sub>60</sub>-based materials, with still unexplored physical and chemical properties.

Although the stability of fullerene in its cationic form was confirmed by cyclic voltammetry, which clearly showed at least three reversible oxidation states,<sup>13</sup> the difficulties arising on oxidizing C<sub>60</sub> in the solid state are not trivial and depend mainly on two factors. On the one hand, the high redox potential of C<sub>60</sub> (+1.26 and +1.71 V for the first and second oxidation,

<sup>†</sup> Università di Parma.

<sup>‡</sup> Institut Laue Langevin.

<sup>§</sup> Physical Chemistry Laboratory, ETH-Zurich.

<sup>||</sup> Laboratorium für Festkörperphysik, ETH-Zurich.

- Holczer, K.; Klein, O.; Huang, S. M.; Kaner, R. B.; Fu, K. J.; Whetten, R. L.; Diederich, F. *Science* **1991**, *252* (5009), 252–257.
- Forro, L.; Mihaly, L. *Rep. Prog. Phys.* **2001**, *64* (5), 649–699.
- Ganin, A. Y.; Takabayashi, Y.; Khimiyak, Y. Z.; Margadonna, S.; Tamai, A.; Rosseinsky, M. J.; Prassides, K. *Nat. Mater.* **2008**, *7* (5), 367–371.
- Takabayashi, Y.; Ganin, A. Y.; Jeglic, P.; Arcon, D.; Takano, T.; Iwasa, Y.; Ohishi, Y.; Takata, M.; Takeshita, N.; Prassides, K.; Rosseinsky, M. J. *Science* **2009**, *323* (5921), 1585–1590.
- Allemand, P. M.; Khemani, K. C.; Koch, A.; Wudl, F.; Holczer, K.; Donovan, S.; Gruner, G.; Thompson, J. D. *Science* **1991**, *253* (5017), 301–303.
- Riccò, M.; Belli, M.; Mazzani, M.; Pontiroli, D.; Quintavalle, D.; Janossy, A.; Csanyi, G. *Phys. Rev. Lett.* **2009**, *102* (14), 145901–4.
- Xie, Q.; Perez-Cordero, E.; Echegoyen, L. *J. Am. Chem. Soc.* **1992**, *114* (10), 3978–3980.

(8) Paci, P.; Cappelluti, E.; Grimaldi, C.; Pietronero, L.; Strässler, S. *Phys. Rev. B* **2004**, *69* (2), 024507.

(9) Lüders, M.; Manini, N.; Gattari, P.; Tosatti, E. *Eur. Phys. J. B* **2003**, *35* (1), 57–68.

(10) Granath, M.; Östlund, S. *Phys. Rev. B* **2002**, *66* (18), 180501.

(11) Reed, C. A.; Bolskar, R. D. *Chem. Rev.* **2000**, *100* (3), 1075–1119.

(12) Reed, C. A.; Kim, K.-C.; Bolskar, R. D.; Mueller, L. J. *Science* **2000**, *289* (5476), 101–104.

(13) (a) Bruno, C.; Doubitski, I.; Marcaccio, M.; Paolucci, F.; Paolucci, D.; Zaopo, A. *J. Am. Chem. Soc.* **2003**, *125* (51), 15738–15739. (b) Bruno, C.; Marcaccio, M.; Castellarin-Cudia, C.; Goldoni, A.; Streltsov, A. V.; Drewello, T.; Barison, S.; Venturini, A.; Zerbetto, F.; Paolucci, F. *J. Am. Chem. Soc.* **2008**, *130* (12), 3788–3796.

versus ferrocene/ferrocenium in TCE solution<sup>7,13</sup>) requires the use of strong oxidants; on the other hand, fullerenes and fullerene cations can easily undergo a nucleophilic attack from anions, which most of the times leads to addition reactions rather than to oxidation, as in fact observed in the case of Br<sub>2</sub> or Cl<sub>2</sub>.<sup>14</sup>

To overcome these difficulties, a possible solution could be the use of the conjugate base of a superacid, which is known to be rather inert and non-nucleophilic, as a consequence of the Hammett acidity function.

In fact, the adoption of the non-nucleophilic carborane-based counteranion CB<sub>11</sub>H<sub>6</sub>X<sub>6</sub><sup>-</sup> (X = Cl, Br), allowed the stabilization of C<sub>60</sub><sup>+</sup> in solution<sup>12</sup> while the activity of the associated Brønsted superacid H(CB<sub>11</sub>H<sub>6</sub>X<sub>6</sub>) (X = Cl, Br) permitted the isolation of HC<sub>60</sub><sup>+</sup> even in the solid state.<sup>12</sup> However, as in the other few cases where C<sub>60</sub><sup>+</sup> could be stabilized in solution,<sup>13</sup> the removal of the solvent invariably led to the degradation of the system,<sup>12</sup> preventing the preparation of a bulk solid compound. The stabilization of a solid fullerenium radical cation was, however, obtained for C<sub>76</sub>,<sup>15</sup> thanks to its lower oxidation potential.

In the present study, the oxidation activity of the Lewis acid AsF<sub>5</sub> proved sufficiently strong to oxidize C<sub>60</sub> to its dication, while both the AsF<sub>3</sub> side product and the counteranion AsF<sub>6</sub><sup>-</sup> generated during the reaction, which is also the conjugate base of the superacid HAsF<sub>6</sub>, proved sufficiently inert and non-nucleophilic to leave the fullerenium ion unattacked.

## 2. Experimental Section

**Synthesis of C<sub>60</sub>(AsF<sub>6</sub>)<sub>2</sub>.** The fullerenium salt C<sub>60</sub>(AsF<sub>6</sub>)<sub>2</sub> was prepared starting from C<sub>60</sub> powder (purity 99.9%, MER Corp.) and gaseous AsF<sub>5</sub> (purity 99.9%, ABCR GmbH), in ratio 1:3; the two compounds were made to react using SO<sub>2</sub> as a solvent (purity 99.9+%, Aldrich). After having dispersed C<sub>60</sub> in liquid SO<sub>2</sub> (previously dried with CaH<sub>2</sub>), the stoichiometric amount of AsF<sub>5</sub> was condensed on this mixture at 77 K in a high-pressure reactor. The system was slowly heated up to 323 K and the mixture was left under continuous stirring for 16 h at a pressure of 8.5 bar. Both the solvent and the volatile reaction products were successively removed by slow evaporation by letting them gurgle into a 1 M NaOH solution. The reaction vessel was then evacuated to a pressure of 10<sup>-2</sup> mbar for 5 min at 273 K. Finally, the sample was removed from the vessel in an Ar glovebox (<1 ppm O<sub>2</sub> and H<sub>2</sub>O). All successive manipulations were done under pure Ar. Due to the high toxicity of both AsF<sub>5</sub> and SO<sub>2</sub>, all the steps of this synthesis must be operated in a suitably designed reactor and by taking all the possible precautions against explosions or possible dispersions of AsF<sub>5</sub>, AsF<sub>3</sub>, and SO<sub>2</sub> gases.

**Structural Analysis.** The diffraction experiments were performed at ambient temperature, respectively, on the ID31 beamline (λ = 0.9337 Å) at the European Synchrotron Radiation Facility (ESRF) and at the SuperD2B diffractometer (λ = 1.59432 Å) at the Institut Laue Langevin (ILL), Grenoble. Gas pycnometry was performed using a home-built pycnometer operating in an Ar glovebox.

**Solid-State MAS and Static NMR Investigation.** MAS NMR spectra were recorded with a Varian Infinity+ 300 spectrometer operating at a <sup>13</sup>C frequency of 75.23 MHz in a Chemagnetics 4 mm double resonance MAS probe. Four-millimeter Chemagnetics rotors were used, whose PTFE inserts were glued to avoid exposure to air. The MAS spectra were collected under a N<sub>2</sub> flow at 298 K, using a spinning frequency of 10 kHz. The reduction of the background signal due to materials outside the coil was achieved

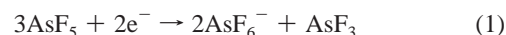
by applying a 180° pulse 50 μs before a 90° pulse on alternate scans and adding and subtracting the resulting FID signals. The <sup>13</sup>C NMR spectra were acquired using 90° pulses of 4 μs duration, a repetition time of 30 s, an acquisition time of 12.8 ms, and a spectral width of 40 kHz. The spectra are the result of the addition of 8000 scans. Continuous wave <sup>19</sup>F-decoupled <sup>13</sup>C spectra were acquired with a decoupling power in the range from 5 to 50 kHz. <sup>13</sup>C NMR spectra were internally referenced to PTFE at 111.3 ppm relative to tetramethylsilane. Static <sup>13</sup>C NMR spectrum and spin–lattice relaxation measurements were performed using an Apollo Tecmag NMR spectrometer, operating at a <sup>13</sup>C frequency of 85.81 MHz, equipped with an Oxford CF-1200 cryostat. Relaxation times were measured via a saturation-recovery pulse sequence, while the static spectrum was registered by a 90°–180° echo sequence, with a 90° pulse width of 3.5 μs and a repetition time of 5 min. The same equipment was also used to record <sup>75</sup>As NMR spectra of the aqueous solution of the sample (see Figure 2S, Supporting Information). The NMR spectra simulations were performed in C++ using the GAMMA spin simulation environment.<sup>16</sup> The powder averaging was performed according to Cheng<sup>17</sup> with 300 powder orientations per spectrum.

**Conductivity Measurements.** Gold metallic contacts were used in the conductivity measurements performed on pressed pellets of the compound. A Keithley 6221 current source and a Keithley 2182A nanovoltmeter, coupled in the delta mode configuration, were used for the resistance measurements. The periodic inversion of the dc current every 0.2 s avoided possible charge accumulations at the electrodes.

**SQUID Magnetometry.** The magnetometry measurements presented in the Supporting Information were carried out using a Quantum Design MPMS-XL5 SQUID magnetometer. The powder sample was sealed in precalibrated quartz ampules and the quartz contribution was canceled by using the background subtraction mode of the instrument.

## 3. Results and Discussion

**Preparation.** The preparation route adopted here is the same as that used in the past to intercalate AsF<sub>6</sub><sup>-</sup> in graphite.<sup>18</sup> This reaction takes place between graphite and AsF<sub>5</sub>, which is known to disproportionate through charge transfer following the scheme



In our case, we performed the reaction of C<sub>60</sub> with AsF<sub>5</sub> by suspending C<sub>60</sub> in liquid SO<sub>2</sub>, where the gaseous AsF<sub>5</sub> is soluble. The oxidation reaction takes place above room temperature at high pressure and follows the scheme



The obtained fullerenium salt remains in suspension as a brown powder and both SO<sub>2</sub> and AsF<sub>3</sub> are efficiently removed by evaporation. Elemental analysis and NMR showed no traces of any of them after vacuum drying the product (see Table 1S and Figure 2S, Supporting Information). The precise control of the AsF<sub>5</sub> stoichiometry and reaction temperature proved essential for obtaining a pure and properly crystallized product. This was not followed in other similar preparations described in the literature.<sup>19</sup> These compounds [referred to as C<sub>60</sub>(AsF<sub>6</sub>)<sub>x</sub>] show

- (14) Taylor, R. *The Chemistry of Fullerenes*; World Scientific: Singapore, 1995; Vol. 4.  
 (15) Bolskar, R. D.; Mathur, R. S.; Reed, C. A. *J. Am. Chem. Soc.* **1996**, *118* (51), 13093–13094.

- (16) Smith, S. A.; Levante, T. O.; Meier, B. H.; Ernst, R. R. *J. Magn. Reson., Ser A* **1994**, *106* (1), 75–105.  
 (17) Cheng, V. B.; Suzukawa, J. H. H.; Wolfsberg, M. *J. Chem. Phys.* **1973**, *59* (8), 3992–3999.  
 (18) Bartlett, N.; McQuillan, B.; Robertson, A. S. *Mater. Res. Bull.* **1978**, *13* (12), 1259–1264.  
 (19) Datars, W. R.; Palidwar, J. D.; Ummat, P. K. *J. Phys. Chem. Solids* **1996**, *57* (6–8), 977–981.

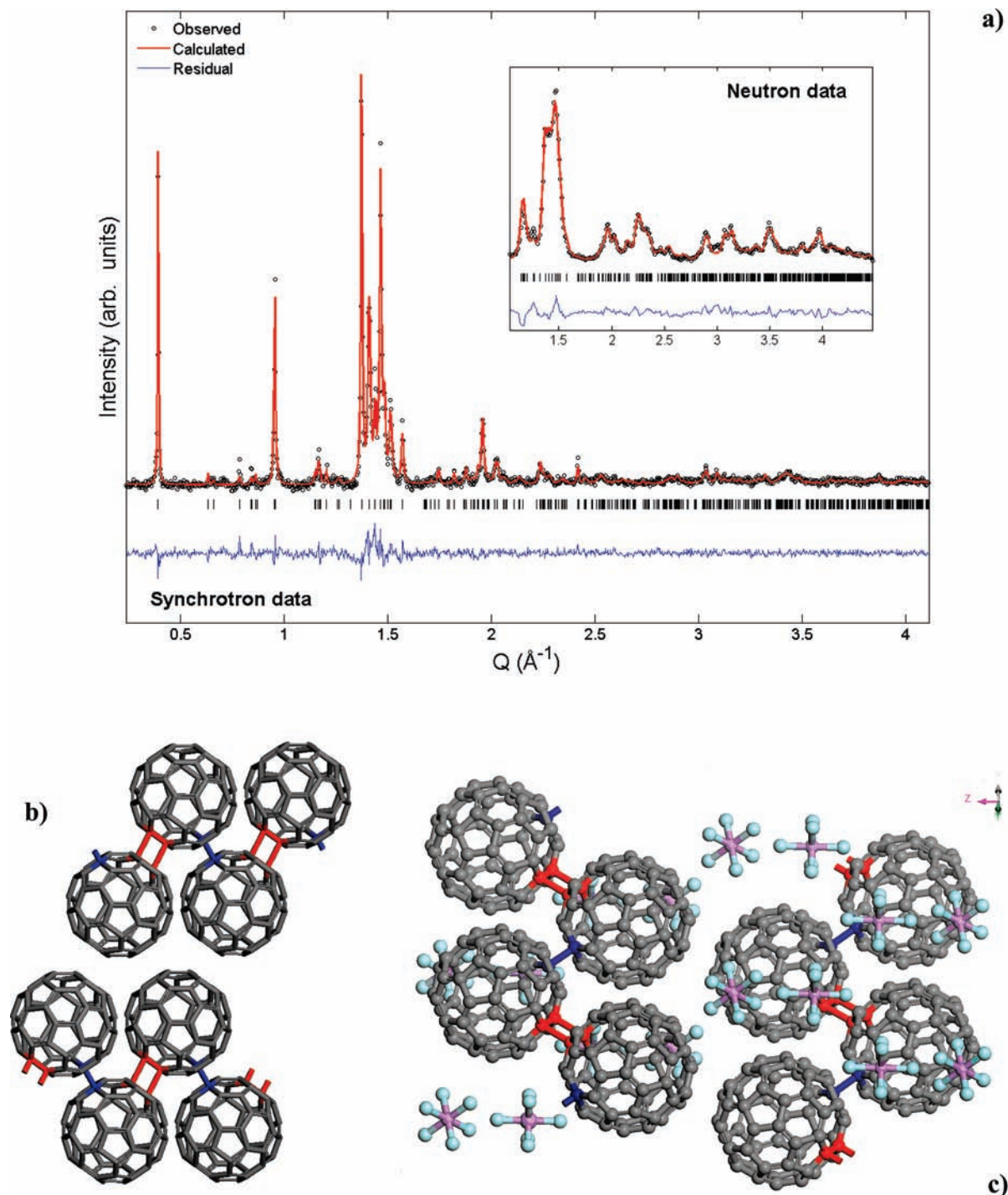


**Figure 1.** (a) Observed (○) and calculated (solid red line) powder diffraction pattern of  $C_{60}(AsF_6)_2$  at 300 K, from synchrotron and neutron diffraction data. (b) The 1D polymeric structure of  $C_{60}(AsF_6)_2$ , consisting of polymeric chains connected alternatively by single C–C bonds and four-membered carbon rings. (c) View of the crystal structure along the (110) crystalline direction.

quite a different diffraction pattern<sup>20</sup> as compared to that reported here and, as suggested by their NMR characterization,<sup>21</sup> probably consist of a mixture of different phases that does not show signatures of polymerization. The obtained salt is very oxygen/moisture sensitive and needs to be handled in pure Ar atmosphere, where it proves to be stable at normal conditions.

(20) Datars, W. R.; Chien, T. R.; Nkum, R. K.; Ummat, P. K. *Phys. Rev. B* **1994**, *50* (7), 4937.

(21) Panich, A. M.; Ummat, P. K.; Datars, W. R. *Solid State Commun.* **2002**, *121* (6–7), 367–370.

**Structural Study and Rietveld Refinement.** Due to the complex structure of the compound, the combination of high-resolution synchrotron and neutron powder diffraction proved necessary to achieve a definitive structural identification of this material. At room temperature both techniques show the presence of a single phase, which we indexed with an orthorhombic cell [ $a = 10.450(3) \text{ \AA}$ ,  $b = 9.993(6) \text{ \AA}$ ,  $c = 32.07(1) \text{ \AA}$ ], although by studying the molecular configuration we proved that the true symmetry is monoclinic (space group  $I2/m$ ) with  $\beta \approx 90^\circ$ . These data and the density of the compound,  $2.2(2) \text{ g/cm}^3$  as

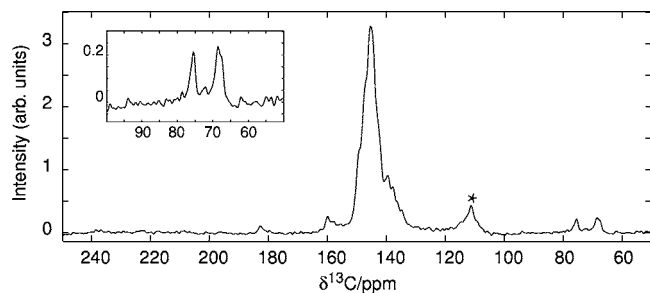


**Figure 2.**  $^{13}\text{C}$  MAS NMR spectrum of the fullerene salt  $\text{C}_{60}(\text{AsF}_6)_2$  collected at room temperature, using a 10 kHz MAS spinning frequency. The inset shows the two peaks in the  $\text{sp}^3$  carbon region. The chemical shifts are relative to TMS. The peak marked with an asterisk is due to PTFE inserts of the rotor.

determined by gas pycnometry, suggest that the correct stoichiometry is  $\text{C}_{60}(\text{AsF}_6)_2$ . We fully confirmed this result by subsequent elemental analysis (optical-ICP) (see Supporting Information). We then achieved the rough structural model of the fullerene salt through the use of a simulated annealing algorithm, after the extraction of the structural factors by whole pattern decomposition (the Pawley method). The best agreement between the observed and calculated data was reached with the  $\text{C}_{60}$  centers of mass at the special position  $4i$  ( $x, 0, z$ ), with  $x = 0.751(1)$  and  $z = 0.1140(8)$ , while the two  $\text{AsF}_6^-$  molecular ions naturally occupy the available empty voids, allowed by the steric hindrance of the fullerenes, centered at the position  $4i$  with  $x = 0.76(2)$ ,  $0.75(2)$  and  $z = 0.700(3)$ ,  $0.558(2)$ . With such an arrangement, the minimum center-to-center distance of two neighboring  $\text{C}_{60}$  units is approximately 9 Å, a value compatible with the polymerization of the molecules.<sup>22</sup> The closest contacts for each fullerene are obtained along two different vectors on the  $ac$  plane, which are not mutually orthogonal.

This generates a “zigzag” disposition of  $\text{C}_{60}$ s, which propagates along the  $a$  crystallographic direction. Remarkably, such a  $\text{C}_{60}$  arrangement in a polymer has never been observed before. The zigzag angle shown by the simulated annealing is  $\sim 72^\circ$ . It is worth noting that such molecular disposition could be easily derived from a distortion of the pristine face-center cubic  $\text{C}_{60}$  network by considering the (1, 1, 1) planes of the cubic lattice: the fullerene units taking part in the polymer chains belong to two contiguous rows of the plane, while the subsequent two rows are replaced by the two couples of  $\text{AsF}_6^-$  ions.

At the same time we performed Rietveld refinement using both synchrotron and neutron data (see Figure 1a): while the former allowed us to localize the various atomic and molecular units within the cell, the latter permitted the determination of the molecular orientation. Some trials using different dispositions, all compatible with the symmetry group  $I2/m$ , allowed us to verify that the agreement factors invariably improve upon orienting the  $\text{C}_{60}$  units, as shown in Figure 1b. This orientation is compatible with the presence of alternated four-membered carbon rings ( $[2 + 2]$  cycloaddition) and single C–C bonds between the fullerene molecules along the zigzag chain.

**Solid-State NMR Spectroscopy and Direct Current Conductivity Measurements.** We further confirmed such an unusual polymer texture by  $^{13}\text{C}$  MAS NMR spectroscopy (Figure 2). The  $^{13}\text{C}$  NMR spectrum of  $\text{C}_{60}(\text{AsF}_6)_2$  consists of a superposition of several resonances at about 140–150 ppm due to  $\text{sp}^2$  carbons

and two well-resolved peaks in the  $\text{sp}^3$  hybridized carbon region, at 68 and 75 ppm. The ratio of the integrals of the peaks at 68 and 75 ppm is about 1:2. This observation is consistent with the presence of two kind of  $\text{sp}^3$  carbons involved in the single and double intermolecular bonds. A similar case has already been observed in the 2D polymer  $\text{Li}_4\text{C}_{60}$ ,<sup>23</sup> where the presence of the two different bonding schemes is also indicated by two distinct  $\text{sp}^3$  peaks. The broad structure of the  $\text{sp}^2$  component is, on the other hand, indicative of the deformation of the  $\text{C}_{60}$  units upon polymerization.  $^{19}\text{F}$ -decoupling did not produce any difference in the  $^{13}\text{C}$  spectrum, thus proving that the  $\text{sp}^3$  carbons are indeed not bonded to fluorine. The electronic properties of the compound can also be inferred from the NMR spectra as, in case of metallic behavior, they would be heavily affected by the Knight shift interaction.

The unresolved multiplet of the several  $\text{sp}^2$  resonances centered at 145 ppm arises from the separate contributions of all the 57  $\text{sp}^2$  carbons of the fullerene molecule which, according to the  $I2/m$  spatial group symmetries, occupy crystallographically nonequivalent positions. As we do not expect large differences in their anisotropic chemical shielding parameters, we adopted a single average shift tensor in the simulation of NMR spectra in the slow MAS or static regime (see Figure 1S, Supporting Information). The resulting parameters, namely an isotropic shift of 145(1) ppm, an anisotropy of  $-110(5)$  ppm, and an asymmetry of 0.2(2), are close in value to those of the chemical shift tensor in pristine  $\text{C}_{60}$ .<sup>24</sup> The onset of a metallic phase would affect the static spectrum by adding a tensorial interaction with the conduction electrons (Knight shift), which is known to possess a positive anisotropy in fullerenes. Its absence suggests the insulating or semiconducting nature of  $\text{C}_{60}(\text{AsF}_6)_2$ .

We obtained further insights into the electronic properties of the new material from  $^{13}\text{C}$  NMR spin–lattice relaxation and dc conductivity measurements. Figure 3 (left panel) represents the  $^{13}\text{C}$  spin–lattice relaxation rate above 80 K, which clearly shows two different regimes: for  $T < 100$  K the  $^{13}\text{C}$  relaxation is dominated by a temperature-independent contribution, most likely originating from the dipolar interaction with localized paramagnetic centers whose presence is evidenced by SQUID magnetometry (see Figure 3S, Supporting Information). These unpaired electronic spins, observed in many fullerene polymers,<sup>25</sup> can be located at polymer structural defects, or at the end of the polymer chains, or, as is more likely in our case, originate from a  $\text{C}_{60}^+$  minor component. For  $T > 100$  K an Arrhenius behavior is observed, with an activation energy  $E_a^{\text{NMR}} = 65$  meV (see inset of Figure 3, left panel). Although a magnetic spin gap could give a similar behavior, the absence of any thermally activated magnetization in the magnetometry data (see Figure 3S, Supporting Information) suggests that the observed increase in relaxation rate could be ascribed to the thermally activated electrons across a small band gap, a clear evidence of semiconducting behavior. Dc conductivity measurements (shown in Figure 3, right panel) confirm this hypothesis. Also the sample conductivity follows an activated behavior and the fitted activation energy,  $E_a^{\text{dc}} = 78.5$  meV, is quite close to the value found from NMR relaxation, hence suggesting that the same process is at the base of the two  $T$  dependences.

(23) Riccò, M.; Shiroka, T.; Belli, M.; Pontiroli, D.; Pagliari, M.; Ruani, G.; Palles, D.; Margadonna, S.; Tomaselli, M. *Phys. Rev. B* **2005**, *72* (15), 155437/1–155437/7.

(24) Sato, N.; Tou, H.; Maniwa, Y.; Kikuchi, K.; Suzuki, S.; Achiba, Y.; Kosaka, M.; Tanigaki, K. *Phys. Rev. B* **1998**, *58* (18), 12433.

(25) Arcon, D.; Zorko, A.; Mazzani, M.; Belli, M.; Pontiroli, D.; Riccò, M.; Margadonna, S. *New J. Phys.* **2008**, *10* (3), 033021.

(22) Chen, X.; Yamanaka, S. *Chem. Phys. Lett.* **2002**, *360* (5–6), 501–508.

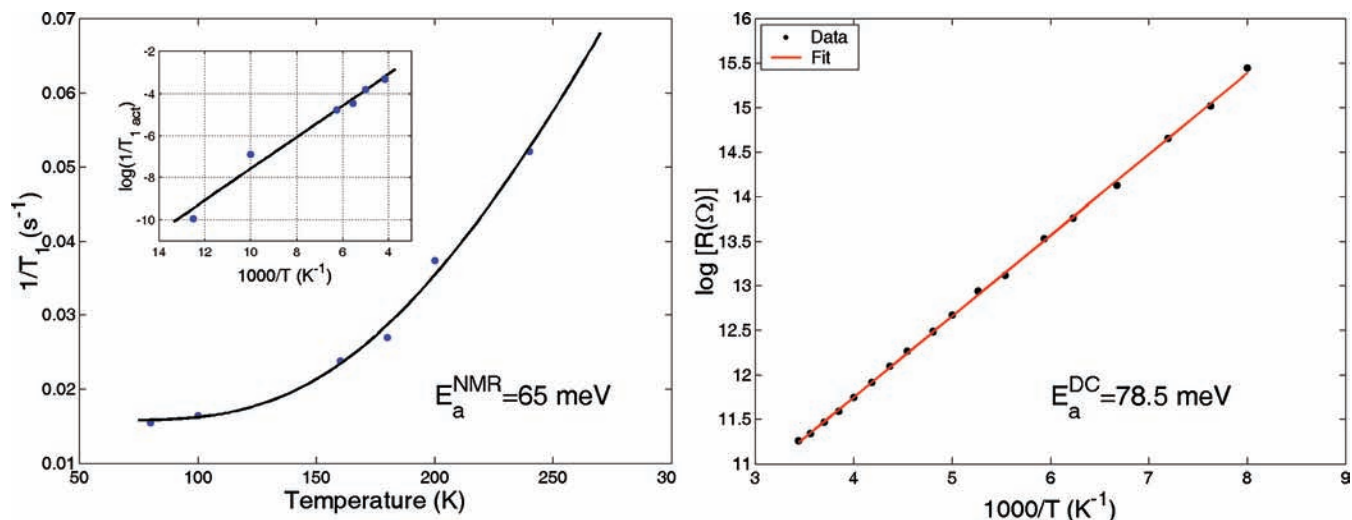


**Figure 3.** Left panel:  $^{13}\text{C}$  NMR spin–lattice relaxation rate of  $\text{C}_{60}(\text{AsF}_6)_2$  vs temperature. The curve represents the best fit to an activated Arrhenius law  $1/T_1 = 1/T_{1\text{par}} + 1/T_{10} \exp(-E_a^{\text{NMR}}/k_B T)$  with activation energy  $E_a^{\text{NMR}} = 65$  meV (see the text). Inset: Arrhenius plot highlighting the activated behavior of relaxation. Right panel: Temperature dependence of dc resistance of pelletized  $\text{C}_{60}(\text{AsF}_6)_2$ . The line represents a fit to an Arrhenius law  $R(T) = R_0 \exp(-E_a^{\text{dc}}/k_B T)$ .

**Discussion.** The large variety of properties displayed by the alkali-intercalated fullerenes, which include also superconductivity (SC) and magnetism with rather high transition temperatures (for a carbon based material), have stimulated high expectations on the potentially promising features of the corresponding  $\text{C}_{60}$  hole-doped compounds. In fact, due to the higher density of states (DOS) at the Fermi energy of the 5-fold degenerate  $h_{1u}$  HOMO derived band in cationic fullerenes, as compared to the 3-fold degenerate LUMO band involved in their anionic counterparts, a substantial increase of the critical temperature is predicted in a hypothetical superconducting fullerene compound.<sup>10</sup> On the basis of these expectations and using a gate-induced doping in a field-effect transistor, Schon and co-workers reported SC at 52 K in hole-doped  $\text{C}_{60}$ ,<sup>26</sup> which raised to 117 K in the expanded hole-doped  $\text{C}_{60}/\text{CHBr}_3$ .<sup>27</sup> These results influenced a relevant part of the scientific community, before the authors were accused of misconduct and the articles successively retracted.<sup>28</sup> In the light of our evidence that the extreme reactivity of  $\text{C}_{60}^{2+}$  ions triggers the formation of intermolecular bonds, it is reasonable to conjecture that also in these first attempts the hole-doped  $\text{C}_{60}$  was in a polymeric state and, consequently, hardly superconducting. A recent, and more reliable, theoretical study predicts a magnetic ground state in an isolated  $\text{C}_{60}^{2+}$  molecular ion, resulting from the competition of Jahn–Teller and Coulomb intramolecular exchange interactions.<sup>9</sup> Actually, we did not observe this expected magnetic state in our  $\text{C}_{60}^{2+}$  cations (see Figure S3, Supporting Information), probably due to the perturbation of the electronic and vibrational properties of the isolated molecular ion introduced by the intermolecular bonds. In fact, no signs of triplet states in  $\text{C}_{60}(\text{AsF}_6)_2$  emerge from SQUID magnetometry. Conversely, as shown by the field dependence of the low- $T$  magnetization (inset of Figure S3, Supporting Information), the observed Curie component is due to  $S = 1/2$ , and it is likely to be attributed to a minor component of  $\text{C}_{60}^+$  entrapped in the polymer lattice. In contrast with other 1D polymerized  $\text{C}_{60}$  compounds, such as  $\text{AC}_{60}$  ( $A = \text{K}, \text{Rb}$ ),<sup>29</sup> which show a metallic behavior at room temperature,  $\text{C}_{60}(\text{AsF}_6)_2$  behaves like a small gap semiconductor,

as evidenced by both  $^{13}\text{C}$  spin–lattice relaxation and by dc conductivity. The energy gap is, however, rather small if compared to other  $\text{C}_{60}$ -based insulating polymers,<sup>30</sup> such a small value indicating the proximity to a metallic phase which can be reached through a continuous insulator-to-metal transition (e.g., induced by the application of external pressure). Alternative explanations of the reported NMR and conductivity results, based on the thermal excitation of localized states within a larger gap,<sup>25</sup> cannot be entirely ruled out and could possibly coexist with the activated electron hypothesis.

#### 4. Conclusions

We have successfully synthesized the fullerene salt  $\text{C}_{60}(\text{AsF}_6)_2$ , where  $\text{C}_{60}$  is present in its dication form. Its solid-state structure studied by combined synchrotron radiation X-ray diffraction and neutron diffraction evidences the polymerization of the  $\text{C}_{60}$  units with an unusual zigzag bonding motif. Although the low nucleophilic propensity of  $\text{AsF}_6^-$  allows the stabilization of  $\text{C}_{60}^{2+}$  in the solid state, the extremely high reactivity of the dication is certainly at the origin of the observed polymerization. This effect puts in doubt the possibility that a monomer fullerene salt with enhanced superconducting and/or magnetic properties (as theoretically predicted in several studies<sup>8–10</sup> and in few cases also claimed<sup>26,27</sup>) could be successfully produced. The synthesized material is, on the other hand, a small gap semiconductor which shows a weak molecular diamagnetism.

**Acknowledgment.** We thank the ESRF and ILL for provision of beamtime and we acknowledge financial support from the EC FP6-NEST Ferrocyanide project. We are grateful to Matthias Ernst, Matteo Belli, and Gianluca Calestani for helpful discussions.

**Supporting Information Available:** Elemental analysis, synchrotron and neutron powder diffraction, Rietveld analysis,  $^{13}\text{C}$  NMR spectroscopy,  $^{75}\text{As}$  NMR spectroscopy, and SQUID magnetometry. This material is available free of charge via the Internet at <http://pubs.acs.org>.

(26) Schon, J. H.; Kloc, C.; Batlogg, B. *Nature* **2008**, *408* (6812), 549–552.

(27) Schon, J. H.; Kloc, C.; Batlogg, B. *Science* **2001**, *293* (5539), 2432–2434.

(28) Schon, J. H.; Kloc, C.; Batlogg, B. *Nature* **2003**, *422* (6927), 93.

(29) Khazeni, K.; Hone, J.; Chopra, N. G.; Zettl, A.; Nguyen, J.; Jeanloz, R. *Appl. Phys. A: Mater. Sci. Process.* **1997**, *64* (3), 263–269.

JA909614X

(30) Macovez, R.; Savage, R.; Venema, L.; Schiessling, J.; Kamaras, K.; Rudolf, P. *J. Phys. Chem. C* **2008**, *112* (8), 2988–2996.